Astron. Astrophys. 339, 215–224 (1998)

ASTRONOMY AND ASTROPHYSICS

Effects of mass flow on resonant absorption and on over-reflection of magnetosonic waves in low β solar plasmas

Á.T. Csík[⋆]**, V.M. Čadež, and M. Goossens**

Center for Plasma-Astrophysics, K.U. Leuven, Celestijnenlaan 200 B, B-3001 Heverlee, Belgium

Received 12 August 1997 / Accepted 23 June 1998

Abstract. The influence of a stationary mass flow on driven resonant MHD waves is studied for incoming slow and fast magnetosonic waves with frequencies in the slow and the Alfvén continua.

In addition to the classic resonant absorption already present in a static plasma, driven resonant waves can also undergo over-reflection. Depending on the strength of the equilibrium flow a variety of resonant MHD wave phenomena comes into existence. The resonant absorption and over-reflection are found for both, slow and fast magnetosonic waves.

The main result of this paper is that even relatively slow flows can have a drastic effect on the behaviour of MHD waves. This is in particular true under solar conditions.

Key words: MHD – plasmas – waves – Sun: atmosphere – Sun: magnetic fields

1. Introduction

It is well known that the solar atmosphere can be highly structured by the magnetic field depending on the solar cycle activity. Commonly observed features such as photospheric flux tubes, coronal holes, magnetic arcades indicate the existence of pronounced local nonuniformities at their boundaries. The nonuniformities are often in the form of transitional layers that separate regions of larger extent and with different, comparatively uniform, physical characteristics. Many of these configurations remain quasistationary when observed for time spans much shorter than their life time, such as periods of MHD waves or periodic oscillations existing throughout the solar atmosphere (Tsubaki, 1988). Typical periods found from spectral analyses of various coronal lines in the optical and UV domains are around 2-6 min (Liebenberg & Hoffman, 1974; Egan & Schneeberger, 1979; Koutchmy et al. 1983). Perturbations with higher frequencies of several Hz were detected too (Pasachoff, 1991).

Magnetosonic waves can be generated by turbulent motions in the photosphere and in the chromosphere, by global solar oscillations or by local releases of energy in magnetic reconnection events, for example. These waves are an important means of energy transport from sources of their origin into the ambient atmosphere, while the magnetic structures can duct them in specific directions (Nakariakov & Roberts, 1995 and references therein). The carried energy can be deposited in the medium by dissipation through mechanisms with different efficiencies. For example, the classic viscous or resistive damping of Alfvén waves is found to be a very inefficient way to transform the wave energy into heat if the plasma is uniform and weakly dissipative. This is due to the large values of the viscous and magnetic Reynolds numbers typical for the solar atmosphere. However, a highly efficient mechanism for wave dissipation can occur in nonuniform magnetic plasmas if resonant slow and resonant Alfvén waves can be excited locally.

In ideal MHD, these resonant waves are confined to individual magnetic surfaces and do not interact mutually. Since each magnetic surface has its own local slow and local Alfvén frequency, a nonuniform magnetic plasma can have two continuous ranges of frequencies related to resonant slow waves and to resonant Alfvén waves.

Introduction of dissipation results into coupling between the neighbouring magnetic surfaces. This coupling remains weak for large values of the viscous and the magnetic Reynolds numbers, typical for the solar atmosphere. In this case, local resonant slow oscillations and local resonant Alfvén oscillations are characterized by steep gradients across the magnetic surfaces. Their excitation provides a means for dissipating wave energy in a nonuniform and weakly dissipative plasma in a far more efficient way than in classical resistive or viscous MHD wave damping in a uniform plasma.

Resonant MHD wave damping was first put forward as a possible mechanism for heating the solar corona by Ionson (1978) and was further developed and investigated by many authors like Rae & Roberts (1982), Poedts, Goossens & Kerner (1989, 1990), Sakurai, Goossens & Hollweg (1991a,b), Okretič & Čadež (1991), Goossens & Hollweg (1993), Goossens, Ruderman & Hollweg (1995) and the review paper by Goossens & Ruderman (1996).

The influence of an equilibrium plasma flow on MHD eigenmodes on a transitional layer in presence of the Alfvén resonance was studied by Hollweg, Yang, Čadež & Gaković (1990).

Send offprint requests to: Á.T. Csík

⋆ On leave from Department of Astronomy, Eötvös University Budapest, Ludovika tér 2 H-1083 Budapest, Hungary

They considered incompressible perturbations in Cartesian geometry. A theoretical analysis of driven resonant MHD waves on magnetic flux tubes with a plasma flow was done by Goossens, Hollweg & Sakurai (1992) who derived an appropriate treatment of the Alfvén and the cusp singularities in ideal MHD. Their procedure will be applied in our paper too. Further studies of the resonant wave absorption on magnetic flux tubes with flow were done by Erdélyi & Goossens (1996) and Erdélyi (1996). Some of the effects of a nonuniform equilibrium flow in a planar layer were studied by Csík, Erdélyi & Čadež (1997) who considered resonant absorption of slow MHD waves due to the cusp resonance only. They did not obtain the effect of over-reflection.

In this paper, however, we perform a more complete analysis of resonant absorption in a nonuniform plasma layer with a uniform flow. The incident waves are here slow and fast magnetosonic waves, and they can be absorbed due to Alfvén and slow resonances in the layer. The layer separates two uniform regions, one of which is transparent for the considered MHD waves while the other one is opaque. The difference in amplitudes of the reflected and the incident wave thus results only from processes related to the resonances. The amplitude of the reflected wave may become larger than that of the incoming wave in which case we have over-reflection.

The paper is organized as follows: Introductory statements about MHD waves in a nonuniform medium such as the solar atmosphere, are given in Sect. 1. The equilibrium configuration is described in Sect. 2 while Sect. 3 contains the governing ideal MHD equations and their solutions for linear waves in each of the three distinct regions of our. The computation of the absorption coefficient is presented in Sect. 4, the results with the discussion are given in Sect. 5 while conclusions are found in Sect. 6.

2. Stationary equilibrium state

We consider a plasma configuration consisting of two semi-infinite homogeneous regions, separated by a nonuniform layer. The $z-$ axis in a Cartesian coordinate system is perpendicular to the boundaries of the nonuniform plasma layer that are located at $z = 0$ and $z = L$. The basic state quantities depend on the variable z only.

The magnetic field $\boldsymbol{B}_0 = (B_0, 0, 0)$ is assumed homogeneous throughout the whole space while the plasma flow with the velocity $\boldsymbol{U}_0 = (U_0(z), 0, 0)$ parallel to the magnetic field, exists for $z < L$ only:

$$U_0(z) = \begin{cases} U_0 = const, & z \le L \\ 0, & z > L. \end{cases}$$

The flow speed is discontinuous at $z = L$ while the other physical quantities, such as the density $\rho_0(z)$ and the temperature $T_0(z)$, have smooth profiles within the layer.

Since the effect of gravity is ignored in our treatment, the statics of the basic state is simply given by:

$$\frac{d}{dz}\left(p_0 + \frac{B_0^2}{2\mu}\right) = 0.$$

This means that the thermal pressure p_0 is uniform due to the assumption B_0 =const, and that we can freely specify either the plasma density $\rho_0(z)$ or the temperature $T_0(z)$. For analytical and numerical reasons, we prescribe the $z-$dependence of the cusp speed $v_c(z)$ instead, and express the other basic state quantities in terms of $v_c(z)$.

The square of the cusp speed is defined in terms of squares of the Alfvén speed $v_A^2(z) \equiv B_0^2/(\mu_0\rho_0(z))$ and of the speed of sound $v_s^2(z) \equiv \gamma p_0/\rho_0(z)$ as

$$v_c^2(z) = \frac{v_A^2 v_s^2}{v_A^2 + v_s^2} = \frac{2}{2+\gamma\beta} v_s^2(z) = \frac{\gamma\beta}{2+\gamma\beta} v_A^2(z). \tag{1}$$

Here, γ is the ratio of specific heats while β is the ratio of the thermal to the magnetic pressure:

$$\beta \equiv \frac{p_0}{p_m} = \frac{2v_s^2}{\gamma v_A^2} \tag{2}$$

with $p_m \equiv B_0^2/(2\mu_0)$. Clearly, β =const in our model.

The squares of the Alfvén and of sound speed, the plasma density and the plasma temperature can be written in terms of $v_c^2(z)$ as:

$$\begin{aligned} &v_A^2(z) = \left(1 + \tfrac{2}{\gamma\beta}\right) v_c^2(z), \quad v_s^2(z) = \left(1 + \tfrac{\gamma\beta}{2}\right) v_c^2(z), \\ &\rho_0(z) = \frac{\rho_0(0) v_c^2(0)}{v_c^2(z)}, \quad T_0(z) = \frac{T_0(0)}{v_c^2(0)} v_c^2(z). \end{aligned} \tag{3}$$

To reduce the mathematical complications as much as possible but still keep the basic physics in our analysis, we consider a simple linear profile for the cusp speed:

$$v_c(z) = \begin{cases} v_1 = const, & z < 0, \\ v_1 - \frac{v_1 - v_2}{L} z, & L \ge z \ge 0, \\ v_2 = const, & z > L. \end{cases} \tag{4}$$

The basic state profiles (3) are prescribed by the values of v_1 and v_2 in Eq. (4) for the cusp speed. However, the speeds v_1 and v_2 are not convenient from a practical point of view as they cannot be estimated in a straightforward way. For this reason, we express them in terms of β and the temperature ratio $r_T \equiv T_0(L)/T_0(0)$ of the two uniform regions as follows:

$$v_1^2 = \frac{\gamma\beta}{2+\gamma\beta} v_A^2 \quad \text{and} \quad v_2^2 = \frac{\gamma\beta}{2+\gamma\beta} r_T v_A^2. \tag{5}$$

In our model, we assume $r_T < 1$ i.e. $\rho_0(L) > \rho_0(0)$ and $v_1 > v_2$. Region 1 ($z < 0$) is thus warmer but less dense than region 2 ($z > L$).

3. Governing equations and solutions

A linear magnetosonic wave with a prescribed frequency ω and wave vector $\boldsymbol{k}$ is launched from the uniform domain $z > L$ (region 2) and it propagates towards the nonuniform layer, in the negative $z-$direction. When the wave enters the nonuniform layer, its characteristics change depending on the wave parameters and on the values of the basic state quantities.

In what follows, we restrict the investigation to those waves that cannot propagate through region 1 i.e. to the waves for which region 1 is nontransmitting.

Fluid motions driven by these incoming waves are described by the standard set of linearized equations of ideal MHD:

$$\begin{aligned}
&\frac{\partial \rho_1}{\partial t} + \nabla \cdot (\rho_0 \boldsymbol{v}_1) + \boldsymbol{U}_0 \cdot \nabla \rho_1 = 0,\\
&\rho_0 \frac{\partial \boldsymbol{v}_1}{\partial t} + \rho_0 (\boldsymbol{U}_0 \cdot \nabla)\boldsymbol{v}_1 + \rho_0 (\boldsymbol{v}_1 \cdot \nabla)\boldsymbol{U}_0 = -\nabla p_1\\
&\quad + \frac{1}{\mu_0}(\nabla \times \boldsymbol{B}_1) \times \boldsymbol{B}_0 + \frac{1}{\mu_0}(\nabla \times \boldsymbol{B}_0) \times \boldsymbol{B}_1,\\
&\frac{\partial \boldsymbol{B}_1}{\partial t} = \nabla \times (\boldsymbol{v}_1 \times \boldsymbol{B}_0) + \nabla \times (\boldsymbol{U}_0 \times \boldsymbol{B}_1),\\
&\frac{\partial p_1}{\partial t} + \boldsymbol{v}_1 \cdot \nabla p_0 + \boldsymbol{U}_0 \cdot \nabla p_1\\
&\quad = v_s^2 \left(\frac{\partial \rho_1}{\partial t} + \boldsymbol{v}_1 \cdot \nabla \rho_0 + \boldsymbol{U}_0 \cdot \nabla \rho_1\right),
\end{aligned} \tag{6}$$

where the subscripts '0' and '1' denote the equilibrium quantities and their Eulerian perturbations respectively.

As the equilibrium quantities depend on z only, the perturbed quantities can be Fourier analyzed with respect to the ignorable spatial coordinates x and y by taking them proportional to $exp[i(k_x x + k_y y)]$. Since we treat a stationary steady state of driven motions excited by an incoming wave with prescribed frequency ω, the time dependency of all perturbed quantities is given by $exp(-i\omega t)$. The perturbed quantities have therefore the following form:

$$f_1(x, y, z, t) = f(k_x, k_y, \omega; z)\mathrm{e}^{i(k_x x + k_y y - \omega t)}.$$

Eqs. (6) can be reduced to two coupled ordinary differential equations for the normal component of the Lagrangian displacement $\xi_z \equiv i\, v_z/\Omega$, where $\Omega \equiv \omega - k_x U_0$, and for the Eulerian perturbation of the total pressure $P \equiv p_1 + B_0 B_{1x}/\mu_0$:

$$D\frac{d\xi_z}{dz} = -C_1 P, \qquad \frac{dP}{dz} = C_2 \xi_z. \tag{7}$$

The coefficient functions $D(z)$, $C_1(z)$, and $C_2(z)$ are given by

$$\begin{aligned}
D &= \rho_0 (v_s^2 + v_A^2)(\Omega^2 - \omega_c^2)(\Omega^2 - \omega_A^2),\\
C_1 &= (\Omega^2 - \omega_A^2)(\Omega^2 - \omega_s^2) - \Omega^2 v_A^2 k_y^2,\\
C_2 &= \rho_0 (\Omega^2 - \omega_A^2).
\end{aligned} \tag{8}$$

Here $\omega_A \equiv k_x v_A$, $\omega_s \equiv k_\parallel v_s$ and $\omega_c \equiv k_x v_c$ are the Alfvén, the sound and the cusp frequency respectively, while $k_\parallel \equiv \sqrt{k_x^2 + k_y^2}$ is the component of the wave vector parallel to the plane of the layer.

The set of ordinary differential equations (7) has two mobile regular singularities at positions where $D(z)$ vanishes in (8):

$$\Omega = \pm\omega_c(z_c) \quad \text{or} \quad \Omega = \pm\omega_A(z_A). \tag{9}$$

Since $\omega_c(z)$ and $\omega_A(z)$ are functions of z, the relations (9) define two continuous ranges of frequencies referred to as the slow continuum and the Alfvén continuum respectively.

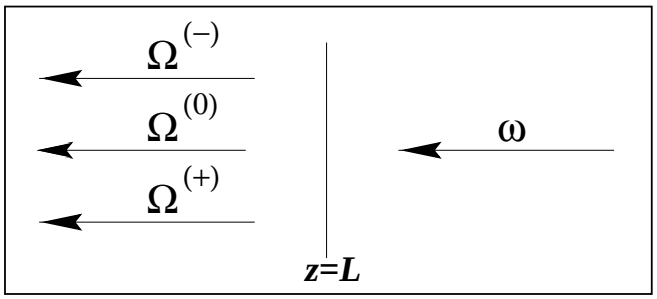

Fig. 1. A schematic wave frequency 'change' from ω to Ω at the boundary separating two regions where plasma is moving and at rest. The superscript of Ω indicates whether the value of $k_x U_0$ is positive, zero or negative.

The existence of these singularities means that the initial assumption of ideal MHD is not valid inside domains localized around each of the resonant points. Dissipative processes cease to be negligible there, they have to be taken into account. The Alfvén and the cusp singularity lead to resonant phenomena of absorption and over-reflection of MHD waves. The details of how dissipation is taken into account in the domains with singularities, are given later in the text.

Eqs. (7) with coefficients (8) indicate that the inclusion of the equilibrium flow U_0 causes only a replacement of frequency ω by a Doppler shifted frequency Ω in the corresponding equations for the linear waves superimposed on a static equilibrium. Thus, when the incoming wave of frequency ω enters the transitional layer with the flow, it behaves there in the same way as would a wave of frequency Ω when the flow is absent. Formally speaking, we are now dealing with a static model in which the wave frequency suffers a jump from ω to Ω at $z = L$. Moreover, the frequency Ω can be negative, contrary to the frequency ω which is always positive. Such a viewpoint simplifies the analysis of the wave propagation characteristics and it will be used in our paper.

The formal frequency change at $z = L$ is shown in Fig. 1: the shifted frequency Ω can be larger, equal or smaller than the initial frequency ω, depending on whether the shift $k_x U_0$ is negative, zero or positive respectively.

To visualize the various possibilities, we give schematic profiles of the characteristic frequencies in Fig. 2. The shaded areas in Fig. 2 designate the frequency domains where waves cannot propagate as their amplitudes are evanescent. However, in the nonuniform layer a wave can partially tunnel through a shaded, nontransparent section separates two propagating domains.

The positive frequency of the incoming fast/slow magnetosonic wave is represented by a solid arrow in region 2. As mentioned above, the effect of the flow corresponds to a formal frequency jump at $z = L$ from ω of the incoming wave to a new value Ω related to one of the white horizontal arrows in Fig. 2, depending on the value of $k_x U_0$. The solid and the dashed parts of these arrows indicate propagating and evanescent waves respectively. The locations of Alfvén and slow resonances are marked by solid and empty squares respectively.

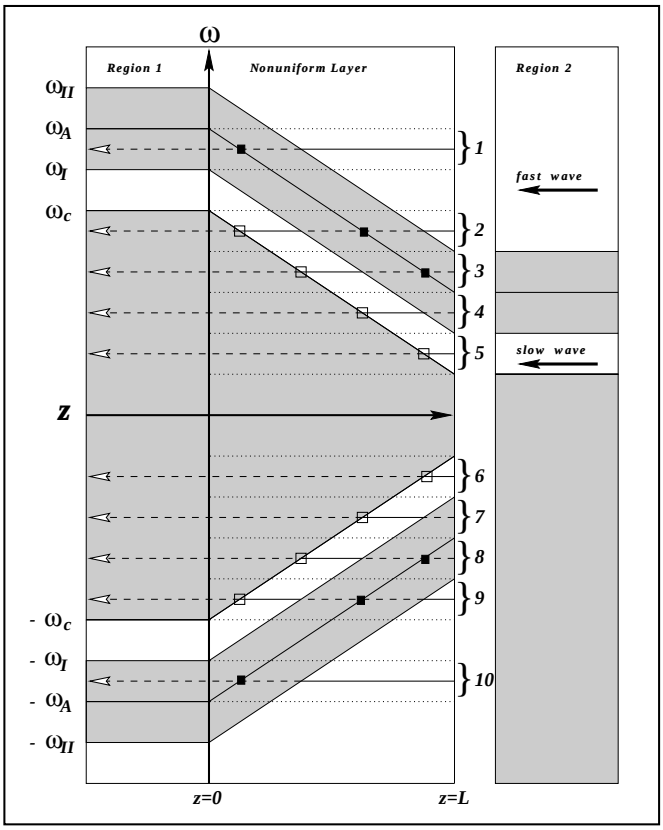

Fig. 2. Schematic profiles of characteristic wave frequencies of the considered model: $\omega_A(z)$, $\omega_c(z)$, $\omega_I(z)$ and $\omega_{II}(z)$ are the local Alfvén, cusp, lower and upper cutoff frequency respectively. At $z = L$, the frequency of the incoming (fast/slow) wave formally changes from ω to Ω located within one of ten indicated intervals related to typical conditions for wave propagation inside the layer. The solid and the dashed parts of horizontal arrows indicate propagating and evanescent waves respectively. Locations of Alfvén and slow resonances are marked by solid and empty squares respectively.

The frequency intervals labeled from 1 to 10 in Fig. 2, represent typical cases of interest in our further treatment. For example, if Ω is in domain 2, we have a wave that propagates over some distance as it enters the layer, then tunnels, reaches the location of the Alfvén resonance and tunnels further up to the next propagating domain. The wave then propagates towards the location of the cusp resonance and becomes evanescent from thereon.

3.1. Solutions in uniform regions

The solutions to Eqs. (7) can be obtained in closed analytic form for a uniform equilibrium state since the coefficients (8) i.e. D, C_1 and C_2, are constants then. In this case, it is straightforward to write Eqs. (7) as a single ordinary differential equation of the second order for P:

$$\frac{d^2P}{dz^2} + \frac{C_1C_2}{D}P = 0. \tag{10}$$

The solutions of Eq. (10) have an exponential $z-$dependence of the form $\exp(ik_z z)$ where the square of k_z is given by:

$$k_z^2 \equiv \frac{C_1C_2}{D} = \frac{(\Omega^2-\omega_I^2)(\Omega^2-\omega_{II}^2)}{(v_A^2+v_s^2)(\Omega^2-\omega_c^2)}. \tag{11}$$

The frequencies ω_I and ω_{II} are the cut-off frequencies for slow and fast magnetosonic waves in a uniform plasma. Their squares are given by

$$\omega_{I,II}^2 = \tfrac{1}{2}(v_A^2+v_s^2)(k_x^2+k_y^2) \times \left\{1 \mp \left[1 - \frac{4\omega_c^2}{(v_A^2+v_s^2)(k_x^2+k_y^2)}\right]^{1/2}\right\}, \tag{12}$$

which yields the following frequency ordering:

$$\omega_{II}^2 \geq \omega_A^2 \geq \omega_I^2 \geq \omega_c^2.$$

3.1.1. Region 1; $z \leq 0$

As wave transmission through the nonuniform layer is not considered in this paper, we restrict the analysis to waves that are evanescent in region 1. The choice of k_x, k_y and Ω should then provide negative values for k_z^2 in Eq. (11) and the required evanescent solution of Eq. (10) is

$$P = \mathrm{e}^{\kappa z} \qquad \text{where} \qquad \kappa^2 \equiv -k_z^2. \tag{13}$$

The integration constant in (13) is fixed by the normalization condition $P(0) = 1$.

The corresponding solution for ξ_z follows from Eq. (7) as

$$\xi_z = \frac{\kappa}{C_2}\mathrm{e}^{\kappa z}. \tag{14}$$

3.1.2. Region 2; $z \geq L$

In region 2, where the equilibrium state is static with $U_0 = 0$, the waves propagate in both directions towards and away from the nonuniform layer. This means that the choice of the values for k_x, k_y and Ω ($= \omega$) have to yield positive values for k_z^2 in expression (11).

The solution of Eq. (10) is here a superposition of two waves propagating in opposite directions along the $z-$axis:

$$P = P^{(+)}\mathrm{e}^{ik_z(z-L)} + P^{(-)}\mathrm{e}^{-ik_z(z-L)} \tag{15}$$

where all coefficients are constant and evaluated at $z = L$.

The corresponding solution for ξ_z follows from Eq. (7) as

$$\xi_z = \frac{ik_z}{C_2}P^{(+)}\mathrm{e}^{ik_z(z-L)} - \frac{ik_z}{C_2}P^{(-)}\mathrm{e}^{-ik_z(z-L)}. \tag{16}$$

There are two frequency windows for propagating magnetosonic waves in a uniform plasma, that follow from Eq. (11) for $k_z^2 \geq 0$. They are

$$\omega_I^2 \geq \omega^2 \geq \omega_c^2 \qquad \text{and} \qquad \omega^2 \geq \omega_{II}^2$$

for slow magnetosonic waves and for fast magnetosonic waves respectively.

A particular property of a slow magnetosonic wave is that the z-components of its phase velocity, $V_{pz} \equiv \omega/k_z$, and of its group velocity, $V_{gz} \equiv \partial\omega/\partial k_z$, have opposite signs. This is evident from their product written as:

$$V_{gz}V_{pz} = \frac{(v_A^2+v_s^2)(\omega^2-\omega_c^2)^2}{(2\omega^2-\omega_I^2-\omega_{II}^2)(\omega^2-\omega_c^2)-(\omega^2-\omega_I^2)(\omega^2-\omega_{II}^2)}.$$

A simple analysis then shows that

$$\begin{aligned} V_{gz}V_{pz} &> 0 \qquad \text{for fast waves,} \\ V_{gz}V_{pz} &< 0 \qquad \text{for slow waves.} \end{aligned} \tag{17}$$

Since the group velocity of a wave is related to the corresponding energy flux, expressions (17) indicate the sense of energy transport with respect to the motion of the wave front, taken along the $z-$axis: the orientations are the same for fast waves and opposite for slow waves.

In an attempt to make the geometry of the wave propagation more visible, we introduce two propagation angles θ and ϕ related to the wave vector and to the magnetic field as:

$$\begin{aligned} &k_x = k\sin\theta\,\cos\phi, \quad k_y = k\sin\theta\,\sin\phi, \\ &k_z = k\cos\theta, \quad k^2 = k_x^2+k_y^2+k_z^2. \end{aligned} \tag{18}$$

Here $\theta \in [0^\circ, 90^\circ]$ is the angle between the wave vector $\boldsymbol{k}$ and the direction of the nonuniformity or the angle of normal incidence, while $\phi \in [0^\circ, 360^\circ]$ is the azimuthal angle or the angle between the magnetic field and the parallel wave vector $\boldsymbol{k}_\parallel \equiv (k_x, k_y, 0)$.

Substitution of expressions (18) into Eq. (11) yields the absolute value of the wave vector:

$$k = \omega\left\{\frac{1}{2}(v_A^2+v_s^2) \pm \frac{1}{2}\left[v_A^4+v_s^4-2v_A^2v_s^2\cos(2\alpha)\right]^{1/2}\right\}^{-1/2}, \tag{19}$$

where

$$\alpha = \text{arc cos}(\sin\theta\,\cos\phi)$$

is the angle between the magnetic field and the wave vector. The plus and the minus sign in Eq. (19) stands for fast and slow magnetosonic wave respectively.

3.2. The nonuniform layer

To solve the system of Eqs. (7), a numerical integration is required in the nonuniform layer. This is done by a simple Runge Kutta Merson scheme starting from values of $P(0)$ and $\xi_z(0)$ at $z = 0$.

As P and ξ_z should be continuous at both boundaries $z = 0$ and $z = L$, the initial values $P(0)$ and $\xi_z(0)$ are obtained from the analytical expressions (13) and (14) for P and ξ_z in region 1, taken at $z = 0$:

$$P(0) = 1 \quad \text{and} \quad \xi_z(0) = \frac{\kappa}{C_2}.$$

Numerical integration of Eqs. (7) is then performed up to the dissipative layer, containing the resonant point, where the ideal MHD approximation becomes unapplicable. The SGHR method developed by Sakurai, Goossens, Hollweg and Ruderman which is described in details in the review article by Goossens & Ruderman (1996), gives the analytical dissipative solutions for P and ξ_z valid in plasma around the resonance. The locations of the end points of this dissipative a layer are estimated from dissipative properties of the medium for each resonance separately.

For our purposes, however, we are not interested in the exact solutions within the dissipative layers and all we need is to know how to connect the ideal solutions between the end points of the layer. This is easily done by the SGHR method which provides us with relevant connection formulae for both P and ξ_z.

In the case of the slow (the cusp) resonance the connection formulae are (Goossens, Hollweg & Sakurai 1992):

$$\begin{aligned} &[\xi_z]_c = -i\pi\,\text{sign}\Omega\frac{\omega_c^4}{|\Delta_c|\rho_0 v_A^2\omega_A^2}P, \\ &[P]_c = 0, \end{aligned} \tag{20}$$

where $\Delta_c = d(\Omega^2-\omega_c^2)/dz$ and all equilibrium quantities in Eq. (20) are taken at $z = z_c$.

The second relation in Eq. (20) represents the conservation law for Eulerian perturbation of total pressure inside the dissipative layer.

The extent of the dissipative layer follows from the asymptotic analysis by Goossens, Ruderman & Hollweg (1995) who estimate it as

$$5\delta_c \geq z - z_c \geq -5\delta_c, \tag{21}$$

where

$$\delta_c = \left(\frac{|\Omega|\eta}{|\Delta_c|}\frac{\omega_c^2}{\omega_A^2}\right)^{1/3}$$

and the isotropic electric resistivity η taken as the dominant dissipative process.

The jump conditions (20) are then applied to connect the numerical values of P and ξ_z across the interval $[z_c-5\delta_c,\ z_c+5\delta_c]$ around the cusp singularity.

In the case of the Alfvén resonance, the connection formulae are (Goossens, Hollweg & Sakurai, 1992):

$$\begin{aligned} &[\xi_z]_A = -i\pi\,\text{sign}\Omega\frac{k_y^2}{|\Delta_A|\rho_0}P, \\ &[P]_A = 0, \end{aligned} \tag{22}$$

where $\Delta_A = d(\Omega^2-\omega_A^2)/dz$.

The corresponding dissipative layer is located at

$$5\delta_A \geq z - z_c \geq -5\delta_A, \tag{23}$$

where

$$\delta_A = \left(\frac{|\Omega|\eta}{|\Delta_A|}\right)^{1/3},$$

while the jumps (22) connect the solutions for P and ξ_z across the interval $[z_A - 5\delta_A,\ z_A + 5\delta_A]$ around the Alfvén singularity at $z = z_A$ (Goossens, Ruderman & Hollweg, 1995).

Once the dissipative layer with the singular point has been crossed, the numerical integration is carried on until the boundary of region 2 is reached at $z = L$ and the related values of $P_L \equiv P(L)$ and $\xi_{zL} \equiv \xi_z(L)$ are obtained.

4. Calculation of the absorption coefficient

To study the resonant absorption of magnetosonic waves, we derive an expression for the absorption coefficient $\mathcal{A}$ from the amplitudes of the incident and the reflected wave at $z = L$.

The absorption coefficient is defined as

$$\mathcal{A} \equiv 1 - \frac{|\mathcal{F}_z^{(r)}|}{|\mathcal{F}_z^{(i)}|}, \tag{24}$$

where $\mathcal{F}_z^{(i)}$ and $\mathcal{F}_z^{(r)}$ are the $z-$components of the energy flux densities of the incident and the reflected wave respectively. $\mathcal{F}_z^{(i)}$ and $\mathcal{F}_z^{(r)}$ can be expressed in terms of the $z-$components of the group velocities $V_{gz}^{(i,r)}$ and the total wave energy densities $w^{(i,r)}$ as

$$\mathcal{F}_z^{(i,r)} = V_{gz}^{(i,r)} w^{(i,r)}. \tag{25}$$

After some algebra (Čadež, Csík, Erdelyi & Goossens, 1997) the expression (24) for the absorption coefficient reduces to

$$\mathcal{A} = 1 - \frac{|P^{(r)}|^2}{|P^{(i)}|^2}. \tag{26}$$

where $P^{(i)}$ and $P^{(r)}$ are amplitudes of total pressure perturbation induced by incident and reflected waves respectively.

The terms 'incident wave' and 'reflected wave' are determined by the sign of the $z-$component of the group velocity in the sense that the incident waves have $V_{gz} \equiv V_{gz}^{(i)} < 0$ while the reflected waves have $V_{gz} \equiv V_{gz}^{(r)} > 0$.

According to inequalities (17), the sign of the z-component of the phase velocity and the z-component of the group velocity are the same for fast magnetosonic waves and opposite for slow magnetosonic waves. Fast magnetosonic waves, therefore, carry energy towards the nonuniform layer while slow magnetosonic waves carry it in the opposite direction. Going back to the solution (15), we see that the amplitudes $P^{(+)}$ and $P^{(-)}$ are related to waves propagating in the positive z-direction and in the negative z-direction respectively. This means that $P^{(+)}$ and $P^{(-)}$ are the amplitudes of the reflected and the incident wave respectively when the wave is fast magnetosonic wave and vice versa for slow waves.

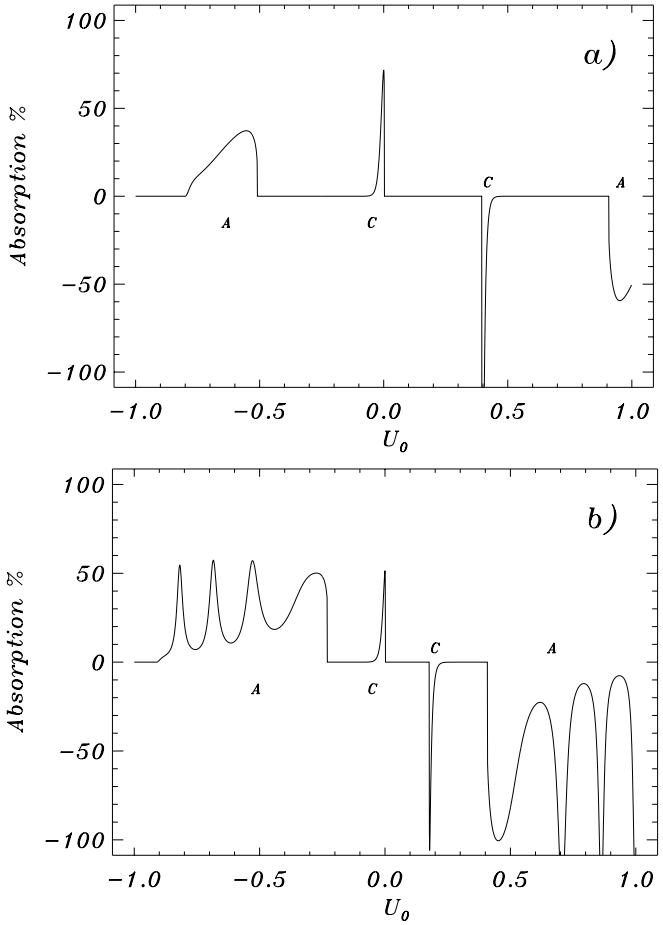

Fig. 3a and b. Model I, slow MHD wave: the dependence of the absorption coefficient on U_0. $\beta = 0.1$, $r_T = 0.5$ (**a**) and $r_T = 0.1$ (**b**).

The amplitudes of the Eulerian perturbation of total pressure $P^{(i)}$ and $P^{(r)}$ for the incident and the reflected wave are

$$\begin{aligned} &P^{(i)} = P^{(-)}, \quad P^{(r)} = P^{(+)} \qquad \text{for fast waves,} \\ &P^{(i)} = P^{(+)}, \quad P^{(r)} = P^{(-)} \qquad \text{for slow waves.} \end{aligned} \tag{27}$$

Finally, applying the boundary conditions of continuity of P and ξ_z at $z = L$ to solutions (15) and (16), we relate the amplitudes $P^{(+)}$ and $P^{(-)}$ to the calculated values P_L and ξ_{zL} from the nonuniform layer as follows:

$$P^{(+)} = \frac{k_z P_L - iC_2\xi_L}{2k_z}, \quad P^{(-)} = \frac{k_z P_L + iC_2\xi_L}{2k_z}. \tag{28}$$

The absorption coefficient (26) is now completely determined by relations (27) and (28) for an incident wave of given frequency ω and propagation angles θ and ϕ.

5. Results and discussion

Numerical calculations are performed with physical quantities normalized as follows: velocities are scaled to $v_{A1} \equiv v_A(0)$, the lengths are are in units of L while the density and the temperature are normalized to $\rho_0(0)$ and $T_0(0)$ respectively.

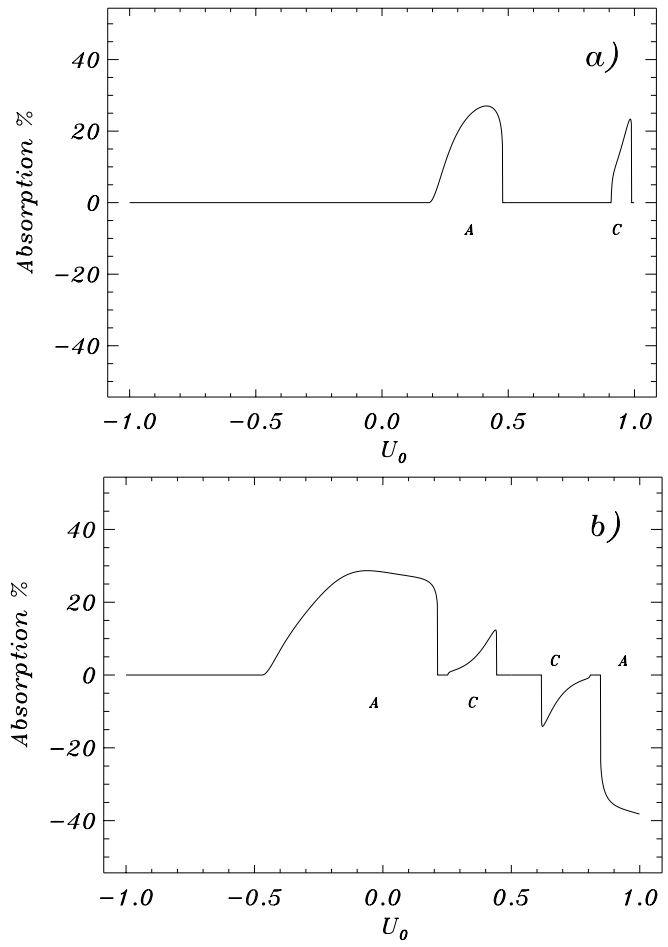

Fig. 4a and b. Model I, fast MHD wave: the dependence of the absorption coefficient on U_0. $\beta = 0.1$, $r_T = 0.5$ (**a**) and $r_T = 0.1$ (**b**).

We consider four different models of the equilibrium state, model Ia, Ib and IIa, IIb. In models I the value of the plasma beta is $\beta = 0.1$, while in models II we take $\beta = 0.01$ which is a better approximation of the higher layers in the solar atmosphere. Each of the models I and II consist of two variants a and b corresponding to the temperature ratios $T_r = 0.5$ and $T_r = 0.1$ respectively. The dimensionless speed of the mass flow is in the interval $U_0 = [-1, 1]$ meaning that we consider flows which are subalfvenic in Region 1.

The aim of this paper is to show, how an equilibrium flow changes the properties of waves with a given frequency and with a given propagation direction. Therefore, we restrict our analysis to waves that enter the nonuniform layer at a prescribed angle of incidence equal to $\theta = 45°$ and at the azimuthal angle $\phi = 30°$. This case assumes $k_y \neq 0$ which allows both for the the cusp and the Alfvén resonance to appear. These particular values for θ and ϕ were chosen because they yield the largest resonant absorption in a static model (Čadež, Csík, Erdélyi and Goossens, 1997). The results presented in this paper are all for incoming waves with dimensionless frequency $\omega = 1$.

Knowing the basic state parameters (5) and the characteristics of the wave, we calculate the absorption coefficient (26) for both slow and fast incoming waves. As said before, we study the absorption of those waves which propagate only through region 2 while they are evanescent in region 1. The absorption coefficient is not calculated if the waves can also propagate in region 1. These cases occur when the shifted frequency Ω falls within one of the following intervals: $|\Omega| \geq |\omega_{II}(0)|$ or $|\omega_c(0)| \leq |\Omega| \leq |\omega_I(0)|$ as seen in Fig. 2.

5.1. Results in models I

Let us first consider the results coming from the interaction of an incoming magnetosonic wave with the nonuniform layer described by model I. In model I $\beta = 0.1$ which can be relevant in the lower parts of the solar atmosphere, like for example the low chromosphere. Figs. 3a and b and 4a and b show the absorption coefficient (26) as a function of U_0 for slow and for fast MHD waves respectively.

Figs. (3a and b) and (4a and b) make it very clear that even a slow equilibrium flow can have a drastic effect on the wave properties. In absence of a flow, i.e. in a static equilibrium, the energy of the wave is partially absorbed by resonant absorption. A small change in the equilibrium flow can remove the positive absorption present in the static equilibrium and even replace it by negative absorption. The negative absorption means that the amplitude of the reflected wave is larger than the amplitude of the incident wave. This phenomenon of over-reflection occurs for both types of waves if the shifted frequency Ω becomes negative and falls within one of intervals $6 - 10$ in Fig. 2. Over-reflection thus exists at positive values of $k_x U_0$ if the Doppler shifted frequency Ω (downwards, in Fig. 1) matches the negative value of the local cusp frequency (intervals $6 - 10$ in Fig. 2):

$$\Omega = -\omega_c(z_c) \quad \text{or} \quad k_x U_0 = \omega + \omega_c(z_c). \tag{29}$$

This requires flows with $U_0 \geq v_c(1) + \omega/k_x$.

The second relation in (29) can be understood as the energy equation in quantum mechanics indicating the flow as the energy source for over-reflection. We point out, that the considered over-reflection and normal wave absorption cannot occur in absence of dissipative losses at resonances.

If Ω takes positive values, which occurs for $\omega = 1 \geq k_x U_0$, the absorption coefficient becomes positive and the incoming wave is partially absorbed. The resonant wave absorption thus occurs for all negative values of $k_x U_0$ and for positive values not exceeding $k_x U_0 = 1$:

$$\Omega = \omega_c(z_c) \quad \text{or} \quad k_x U_0 = \omega - \omega_c(z_c). \tag{30}$$

In Fig. 3a the results are shown for the temperature ratio $T_r = 0.5$. There are four different velocity intervals where the absorption coefficient is nonzero. Going from the left to the right these intervals correspond to the absorption at the Alfvén resonance, absorption at the cusp resonance, over-reflection at the cusp resonance, and over-reflection at the Alfvén resonance, which coincide with domains 1, (4, 5), (6, 7) and 10 in Fig. 2,

respectively. Domains 2, 3, 8 and 9 are not present in our calculations since in model I and II the relation $\omega_c(0) < \omega_A(1)$ is always hold, which means that the cusp and the Alfvén resonances can not occur together for the same value of the flow speed U_0. The labels C and A correspond to the pure cusp and Alfvén resonance, respectively. Absorption and over-reflection occur over a wider interval of velocity for the Alfvén resonance than for the cusp resonance.

Comparison of Fig. 3b with Fig. 3a reveals that the shape of the absorption and the over-reflection curves at the cusp resonance do not change significantly with the temperature ratio. The main difference is that the smaller temperature ratio results smaller peak values for the absorption (from 70 % in Fig. 3a to 50 % in Fig. 3b) and for the over reflection (250 % in Fig. 3a to 100 % in Fig. 3b). In Fig. 3b the absorption and the over-reflection at the Alfvén resonance shows an oscillatory behaviour, and the peak values are larger than in the previous case.

Turning to the fast incoming magnetosonic waves, Figs. 4a and 4b shows the absorption coefficient as a function of the flow speed U_0 for temperature ratios $T_r = 0.5$ and $T_r = 0.1$, respectively. The main conclusion from these figures is that the fast waves are less sensitive to the variation of the flow speed. After a smooth increase the absorption approximately stays on its maximal value and then suddenly drops to zero. Over-reflection is also present, but less prominent than for the slow waves. The oscillatory behaviour is not present in Fig. 4b, just in contrast to Fig. 3b. The change of the temperature ratio does not have a strong influence on the peak values in Figs. 4a and 4b. The main difference between the two figures is that the absorption and the over-reflection take place in different intervals of the flow speed U_0, coming from the fact that the variation of the temperature ratio results in a variation in the width of the cusp and the Alfvén continua. For example, in the case of the temperature ratio $T_r = 0.5$ the given incoming wave even can not be over reflected in the subalfvenic regime since $\Omega > -\omega_c(1)$ is valid for $|U_0| < 1$.

5.2. Results in models II

Model II has $\beta = 0.01$, which is a more realistic value for the plasma beta in the higher solar atmosphere. In Figs. 5a and 5b we present the variation of the absorption coefficient as a function of the flow speed U_0 for the temperature ratios $T_r = 0.5$ and $T_r = 0.1$, respectively.

Comparison of Figs. 5-6 to Figs. 3-4 of model I, leads us to the following conclusions. For slow incoming waves the reduction of β results in a reduction of the peak values for both temperature ratios while its effect on the fast MHD waves is less pronounced. The oscillatory behaviour of the curves at the pure Alfvén resonance is more pronounced in Fig. 5b than in Fig. 3b.

The results for fast incoming waves are shown in Figs. 6a and 6b. The variation of the plasma beta does not have a strong influence on the absortion curves for both temperature ratios. The main difference between Figs. 4ab and Figs. 6ab comes from the slight change of the absorption and over-reflection at the cusp resonance.

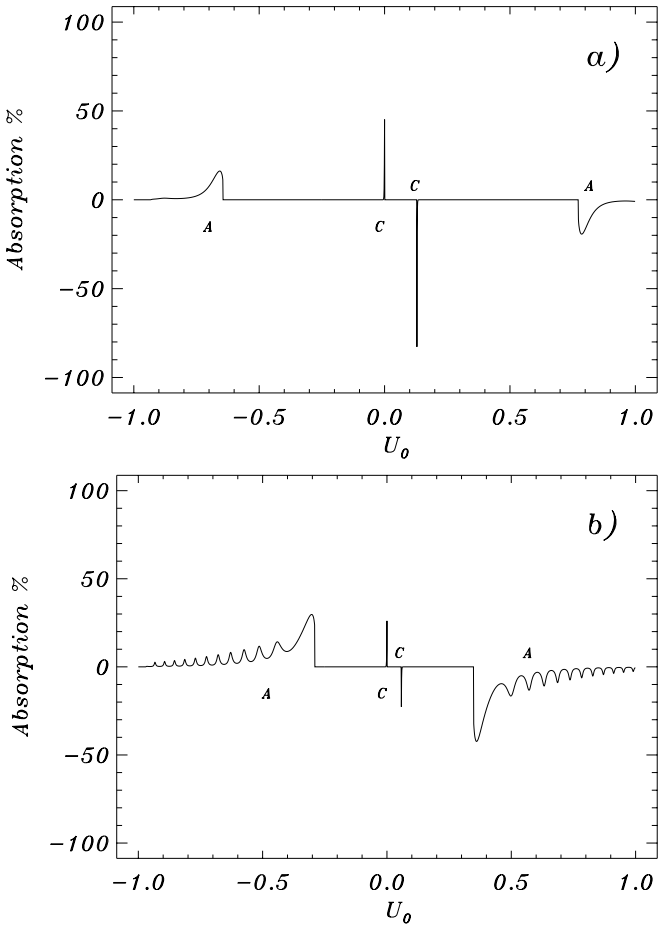

Fig. 5a and b. Model II, slow MHD wave: the dependence of the absorption coefficient on U_0. $\beta = 0.01$, $r_T = 0.5$ (**a**) and $r_T = 0.1$ (**b**).

6. Conclusions

The main aim of this paper is to show that in low β solar plasmas even a slow bulk flow, can have a strong effect on resonant MHD wave absorption and reflection from localized inhomogeneous layers. Numerical calculations were performed for two values of the plasma β ($\beta = 0.1$ and $\beta = 0.01$ relevant to the lower and the higher parts of the solar atmosphere, respectively) and for two values of the temperature ratio $T_r = 0.5$ and $T_r = 0.1$.

The efficiency of absorption of slow MHD waves is the same for the slow and the Alfvén resonance. The fast MHD waves are absorbed much more efficiently at the Alfvén resonance than at the cusp resonance in our models. Additionally, the flow has a strong influence on the variation of the absorption coefficient for slow MHD waves. The variation for the fast MHD waves is much smoother. Finally, in the four cases considered here the peak values are much higher for the slow MHD waves than for the fast MHD waves.

Our results can be applied to processes in the solar atmosphere in a broader sense and with certain restrictions, as commonly done in literature. This means that the physical properties of regions 1 and 2 may in fact apply to local domains of at least

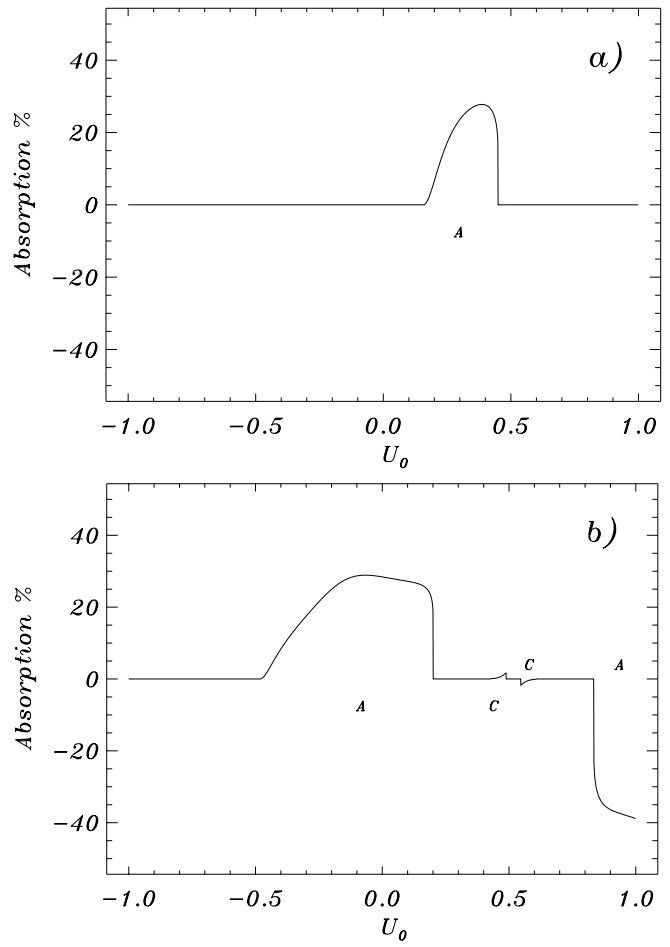

Fig. 6a and b. Model II, fast MHD wave: the dependence of the absorption coefficient on U_0. $\beta = 0.01$, $r_T = 0.5$ (**a**) and $r_T = 0.1$ (**b**).

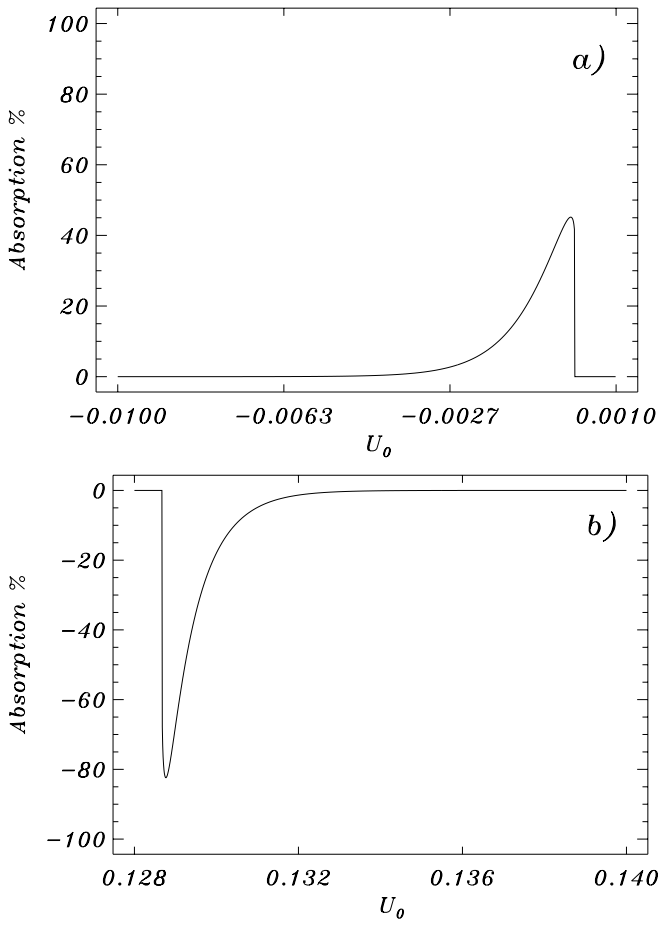

Fig. 7a and b. Model IIa, slow MHD wave: the dependence of the absorption coefficient on U_0. $\beta = 0.01$, $r_T = 0.5$.

several wavelengths on both sides of the nonuniform layer and not necessarily to the whole atmosphere.

Thus, regions 1 and 2 can, in principle, be considered uniform only locally if so needed in applications. Uniformity of regions 1 and 2 is therefore not required on length scales much larger than the wavelength λ. The same holds for the uniform flow meaning that the flow is present throughout the transitional layer but it may be of only local extent in the region 1 where the medium is considered uniform.

In addition, as the effects of the spherical shape of the solar atmosphere and the gravity stratification are not taken into account in our study, the wavelength λ of the plane waves should be much smaller than the solar radius and the typical stratification scale length.

We turn now to applications of our results to solar conditions. Let us take a local inhomogenity in the high chromosphere, which is embraced by two uniform media with temperatures $T_1 = 100.000K$ and $T_2 = 50.000K$ (for example the lower parts of an arcade, where the magnetic field lines are approximately perpendicular to the solar surface). Model IIa is suitable for this case, since $\beta = 0.01$ is a proper value for the plasma beta at this height and the ratio of the temperatures is $T_r = 0.5$.

These temperatures correspond to sound speeds of $v_{s1} = 45$ km s^{-1} and $v_{s2} = 32$ km s^{-1} respectively, which yield $v_{A1} =$ 493 km s^{-1} and $v_{A2} = 350$ km s^{-1} in the two regions. These values fall in the interval (10^2-10^4) km s^{-1} typical for the Alfvén speed in the higher solar atmosphere (Priest, 1985).

The speed of flow U_0 is scaled to v_{A1} and the dimensional values u_0 are then

$$u_0 = 493\, U_0\, [\text{km s}^{-1}]. \tag{31}$$

In solar conditions, realistic values for u_0 are up to $100\, km\, s^{-1}$ (Durrant, 1988) which corresponds to $|U_0| \leq 0.2$.

In Figs. 7ab we present zooms made from the central parts of Fig. 5a. Figs. 7a and 7b show the absorption and the over-reflection for an incoming slow wave, respectively. In model IIa, the choice of $U_0 = 0$ gives $\mathcal{A} = 45\%$ as the value of the absorption coefficient for the static case. Fig. 7a shows, that in the realistic flow interval mentioned above, the absorption can slightly increase up to 48%, and it also can decrease to zero due to the variation of the equilibrium flow.

It is important to show, that in the presented realistic model the slow magnetosonic waves can easily undergo over-

reflection. In Fig. 7b it is shown that a relatively weak flow present in the solar atmosphere is sufficient to increase the energy of the incoming slow wave due to over-reflection. Indeed, a plasma flow in the direction of the magnetic field with speed of 60 km s^{-1} can cause an 80 $\%$ increase of the energy of the incoming slow wave. We would like to point out that the effect of over-reflection can be detected in the solar atmosphere, and it could be a challenging task for the observers community to observe such an interesting phenomenon.

We can now estimate the oscillation period of the wave and the thickness L of the transitional layer. As the dimensional frequency is normalized to the value of v_{A1}/L, the corresponding oscillation period $\mathcal{T}$ is $\mathcal{T}= 2\pi L/(\omega v_{A1})$ where $\omega = 1$ is the dimensionless frequency used in the calculations. If L is given in [km] then $\mathcal{T} = 0.013\, L$/[s] in our case. For example, $L = 500$ km gives oscillation periods of $\mathcal{T} = 6$s.

The conclusion is that the plasma flows expected to be present in the solar atmosphere, can significantly affect the resonant absorption of both types of magnetosonic waves in the observed frequency range. The considered resonant processes occurring in nonuniform layers, can contribute to atmospheric heating. Additionally, we showed that under solar conditions the slow magnetosonic waves can gain significant amount of energy from the existing bulk plasma flows. Later on this energy can be deposited by a following dissipative process, giving a rise to the heating of the solar atmosphere.

Finally, the following remark on over-reflection is in order. The increase of the wave amplitude after the reflection from the layer may also be related to eventual flow instabilities induced by the incident wave. Our basic state model allows, in principle, for two types of instabilities, the Kelvin-Helmholtz instability modified by the presence of the nonuniform layer, and resonant flow instabilities when the conditions (29) and (30) are satisfied. These instabilities were considered by Hollweg, Yang, Čadež & Gaković (1990) in the limit of incompressible fluid. To fully understand the process of over-reflection it is therefore necessary to investigate stability properties of the considered basic state by solving the related eigenvalue problem.

Acknowledgements. V.M.Čadež is grateful to the 'Onderzoeksfonds K.U.Leuven' for awarding him the senior research fellowship (F/97/9). Á. Csík is grateful to the Hungarian Soros Foundation, the "Onderzoeksfonds K.U.Leuven" and to the Hungarian Airlines Company for the financial support. The authors are also thankful to M.Ruderman for valuable discussions on the considered subject.

References

Čadež, Csík, Á., Erdélyi, R. & Goossens, M. 1997, A&A, 326, 1241.
Csík, Á., Erdélyi, R. & Čadež, 1997, Solar Phys., 172, 61.
Durrant, C.J., 1988, The Atmosphere of the Sun, Adam Hilger, Bristol and Philadelphia.
Egan, T.F & Schneeberger, T.J. 1979, Solar Phys., 64, 223.
Erdélyi, R. and Goossens, M. 1996, A&A, 313, 664.
Erdélyi, R. 1996, Resonant Absorption of MHD Waves in Visco-Resistive Plasmas: Applications to the Solar Atmosphere, Ph.D thesis, K.U.Leuven, Leuven, Belgium.
Goossens, M., Hollweg, J. V., & Sakurai, T. 1992, Solar Phys., 138, 233.
Goossens,M. & Hollweg, J.V. 1993, Solar Physics. 145, 19.
Goossens, M., Ruderman, M. S. and Hollweg, J.V. 1995, Solar Phys., 157, 75.
Goossens, M. & Ruderman, M. S. 1996, Physica Scripta, T60, 171.
Hollweg, J.V., Yang, G., Čadež, V.M. & Gaković, B. 1990, ApJ, 349, 335.
Ionson,J.A.: 1978, ApJ. 226, 650.
Koutchmy, S., Zugzda, Y.D. & Locans, V. 1983, A&A, 120, 185.
Liebenberg, D.H. & Hoffman, M.M. 1974, in Coronal Disturbances, ed. G.Newkirk, Jr. (Reidel: Dordrecht), p.485.
Nakariakov, V.M. & Roberts, B. 1995, Solar Phys., 159, 213.
Okretič, V. and Čadež, V.M. 1991, Physica Scripta, 43, 306.
Pasachoff, J.M. 1991, in Mechanisms of Chromospheric and Coronal Heating, eds. P. Ulmschneider, E.R. Priest & R. Rosner (Springer Verlag: Berlin), p. 25.
Poedts, S., Goossens, M. & Kerner, W. 1989, Solar Phys., 123, 83.
Poedts, S., Goossens, M. & Kerner, W. 1990, ApJ, 360, 279.
Priest, E.R. 1984, Solar Magnetohydrodynamics, D.Reidel Publ.Co. Dordrecht, Holland, p.2.
Priest, E.R. 1986, Solar System Magnetic Fields, D.Reidel Publ.Co. Dordrecht, Holland.
Rae, I.C. & Roberts, B. 1982, Monthly Notices Roy. Astron. Soc., 201, 1171.
Sakurai, T., Goossens, M. and Hollweg, J.V. 1991a, Solar Phys., 133, 227.
Sakurai, T., Goossens, M. and Hollweg, J.V. 1991b, Solar Phys., 133, 247.
Tsubaki, T. 1988, in Solar and Stellar Coronal Structures and Dynamics, ed. R.C. Altrock, National Solar Observatory, p. 140.